

Identification and Characterization of Xiamycin A and Oxiamycin Gene Cluster Reveals an Oxidative Cyclization Strategy Tailoring Indolosesquiterpene Biosynthesis

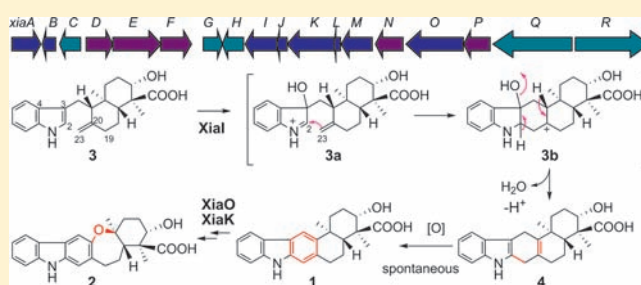
Huixian Li,^{†,§} Qingbo Zhang,^{†,‡,§} Sumei Li,[†] Yiguang Zhu,[†] Guangtao Zhang,[†] Haibo Zhang,[†] Xinpeng Tian,[†] Si Zhang,[†] Jianhua Ju,[†] and Changsheng Zhang^{*,†}

[†]CAS Key Laboratory of Marine Bio-resources Sustainable Utilization, RNAM Center for Marine Microbiology, Guangdong Key Laboratory of Marine Materia Medica, South China Sea Institute of Oceanology, Chinese Academy of Sciences, 164 West Xingang Road, Guangzhou 510301, China

[‡]Graduate University of Chinese Academy of Sciences, 19 Yuquan Road, Beijing, 100049 China

Supporting Information

ABSTRACT: Xiamycin A (XMA) and oxiamycin (OXM) are bacterial indolosesquiterpenes featuring rare pentacyclic ring systems and are isolated from a marine-derived *Streptomyces* sp. SCSIO 02999. The putative biosynthetic gene cluster for XMA/OXM was identified by a partial genome sequencing approach. Eighteen genes were proposed to be involved in XMA/OXM biosynthesis, including five genes for terpene synthesis via a non-mevalonate pathway, eight genes encoding oxidoreductases, and five genes for regulation and resistance. Targeted disruptions of 13 genes within the *xia* gene cluster were carried out to probe their encoded functions in XMA/OXM biosynthesis. The disruption of *xiaK*, encoding an aromatic ring hydroxylase, led to a mutant producing indosespene and a minor amount of XMA. Feeding of indosespene to XMA/OXM nonproducing mutants revealed indosespene as a common precursor for XMA/OXM biosynthesis. Most notably, the flavin dependent oxygenase Xial was biochemically characterized in vitro to convert indosespene to XMA, revealing an unusual oxidative cyclization strategy tailoring indolosesquiterpene biosynthesis.



INTRODUCTION

Indolosesquiterpenes, a group of indole-containing alkaloids, are primarily found as plant metabolites. After the first report of polyalthenol from *Polyalthia oliver*,¹ several plant-derived indolosesquiterpenes have been discovered, including polyveoline,² polyavolinamide,³ greenwayodendrin-3-one,⁴ isopolyalthenol and neopolyalthenol,⁵ 3-farnesylindoles,⁶ and suaveolin-dole.⁷ The most recent examples are polysin⁸ and pentacyclindole.⁹ Fungus-derived indolosesquiterpenes have only been discovered in the past decade, including sespindole and lacinindoles.¹⁰ Cane's pioneering genome mining work suggests actinomycetes to be a prolific resource for terpenoids.¹¹ In accordance with this suggestion, a few indolosesquiterpenes of actinomycete origin have been reported very recently. For example, oridamycins A and B were isolated from a soil *Streptomyces*;¹² a family of indolosesquiterpenes including xiamycin A (XMA, 1, Scheme 1) and xiamycin B, indosespene (3, Scheme 1), and sespenine were reported from two endophytic *Streptomyces* associated with mangrove plants.¹³ In our screening program to discover novel natural products from marine-derived actinomycetes,¹⁴ xiamycin A was reisolated from a marine-derived *Streptomyces* sp. SCSIO 02999, together with four novel indolosesquiterpenes, including oxiamycin (OXM, 2, Scheme 1), chlorox-

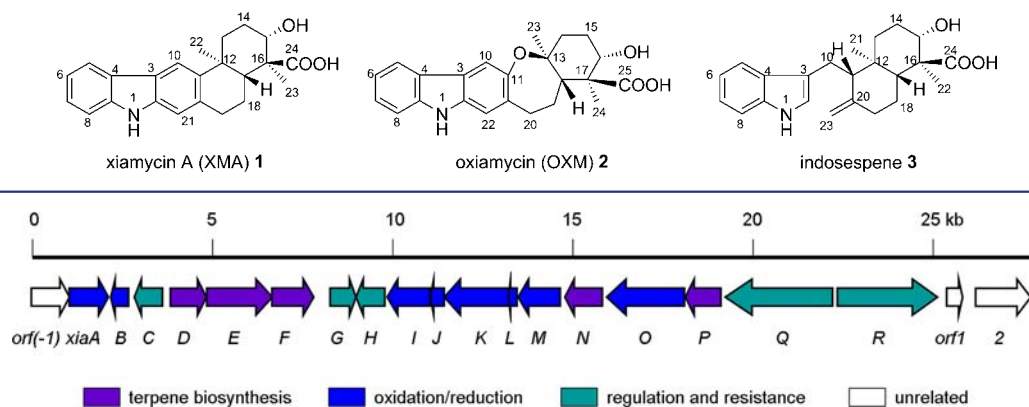
iamycin, and dixiamycins A and B. Oxiamycin contains a 2,3,4,5-tetrahydrooxepine ring, and dixiamycins A and B are two N–N-coupled atropo-diastereomeric dimers of XMA (unpublished results).

Structurally, XMA (1) and OXM (2) are both pentacyclic indolosesquiterpenes containing an indole moiety and a sesquiterpene moiety. Different from XMA (1), the C-11 and C-13 in OXM (2) are bridged by an oxygen atom to form an unusual 2,3,4,5-tetrahydrooxepine ring (Scheme 1). Terpenes are usually assembled from two isomeric five-carbon building blocks, isopentenyl diphosphate (IPP) and dimethylallyl diphosphate (DMAPP), via the mevalonate pathway or non-mevalonate pathway.¹⁵ Sequential condensation reactions of DMAPP with two units of IPP form farnesyl pyrophosphate (FPP), the common precursor dedicated for sesquiterpene biosynthesis. Various terpene synthase catalyzed cyclizations of FPP, followed by a set of tailoring oxidative/reductive modifications, lead to structurally diversified sesquiterpenes in actinomycetes, for example, BE-40644,¹⁶ geosmin,¹⁷ epi-isozizaene,¹⁸ albaflavenone,¹⁹ pentalenolactone,²⁰ and avermilitol.²¹ Biosynthetic mechanisms of these sesquiterpenes have

Received: March 28, 2012

Published: May 16, 2012

Scheme 1. Chemical Structures of Xiamycin A (XMA, 1), Oxiamycin (OXM, 2), and Indosespene (3)

Figure 1. Genetic organization of the *xia* gene cluster. Proposed functions of individual open reading frames (orf's) are labeled and summarized in Table 1.Table 1. Deduced Function of orf's from the *xia* Gene Cluster in *Streptomyces* sp. SCSIO 02999

gene	size in AA ^a	proposed function	protein homologue (accession no.)	homology (% identity/% similarity)
<i>orf(-1)</i>	351	alcohol dehydrogenase	SACTE_6109 (AEN13888)	72/81
<i>xiaA</i>	363	Rieske 2Fe–2S domain-containing oxygenase	SCLAV_0024 (EFG05100)	58/72
<i>xiaB</i>	164	FMN-binding flavin reductase	Strvi_6224 (AEM85702)	76/84
<i>xiaC</i>	258	IcLR family transcriptional regulator	Trd_0252 (ACM04610)	35/49
<i>xiaD</i>	330	HMBPP reductase	Kfla_4244 (ADB33280)	72/79
<i>xiaE</i>	605	DXP synthase	Caci_6415 (ACU75269)	63/73
<i>xiaF</i>	383	HMBPP synthase	IspG (ZP_08876217)	90/95
<i>xiaG</i>	240	LuxR family regulator	Micau_3829 (ADL47353)	55/70
<i>xiaH</i>	266	putative membrane protein	Orf15 (BAD07391)	39/59
<i>xiaI</i>	397	indole oxygenase/acyl-CoA dehydrogenase	Orf5 (AAYS4299)	39/55
<i>xiaJ</i>	129	limonene-1,2-epoxide hydrolase	Swit_5231 (ABQ71340)	37/53
<i>xiaK</i>	597	aromatic ring hydroxylase	RHA1_ro00538 (ABG92374)	52/65
<i>xiaL</i>	77	ferredoxin	SACE_2838 (CAM02117)	59/68
<i>xiaM</i>	389	cytochrome P450	Mjls_0508 (ABN96320)	47/61
<i>xiaN</i>	341	polyprenyl diphosphate synthase	HopB (BAC69362)	52/63
<i>xiaO</i>	718	monooxygenase	SSFG_00177 (EFE64923)	52/64
<i>xiaP</i>	335	polyprenyl synthetase	SSNG_07282 (EFL20030)	44/59
<i>xiaQ</i>	992	LuxR family transcriptional regulator	PlmR5 (AEW92815)	41/50
<i>xiaR</i>	924	LuxR family transcriptional regulator	PlmR4 (AAQ84140)	33/44
<i>orf1</i>	145	zinc metalloprotease	bcere0019_23140 (EEL34460)	35/47
<i>orf2</i>	508	putative sodium-coupled permease	SGM_0166 (EGG49826)	86/91

^aAA, amino acids.

been well characterized at genetic and biochemical levels.^{11,16} Although it was hypothesized that epoxidation and cyclization of a farnesylindole progenitor would lead to the decaline system of indosespene (3), which was further oxidized to form the pentacyclic ring system of xiamycins,^{13b} no biosynthetic studies have been carried out for these newly identified indolosesquiterpenes of actinomycete origin. In this study, we unveiled the first actinobacterial indolosesquiterpene biosynthetic gene cluster for XMA (1)/OXM (2) in marine-derived *Streptomyces* sp. SCSIO 02999 by partial genome sequencing, and confirmed the identity of the gene cluster for XMA/OXM biosynthesis by in vivo gene-disruption experiments. Indosespene (3) was proven to be a common precursor requisite for XMA/OXM biosynthesis. Notably, the flavin dependent oxygenase *XiaI* was found to be capable of transforming indosespene (3) to XMA (1), implicating an unprecedented oxidative cyclization strategy tailoring indolosesquiterpene biosynthesis.

RESULTS

Identification of the *xia* Gene Cluster for XMA/OXM Biosynthesis in *Streptomyces* sp. SCSIO 02999. We utilized a genome sequencing strategy to facilitate the identification of the XMA gene cluster from *Streptomyces* sp. SCSIO 02999. After contig assembly and careful bioinformatic analyses, the putative *xia* gene cluster was localized on a continuous DNA region of ~29 kb (GenBank accession number JQ812811), which comprised 21 open reading frames (orf's) (Figure 1, Table 1). A SuperCos1 genomic library of *Streptomyces* sp. SCSIO 02999 was then constructed and six positive cosmid clones (Table S1 and Figure S1 in the Supporting Information) were identified from around 2400 clones by using a pair of specific polymerase chain reaction (PCR) primers *XiaD*-1F and *XiaD*-1R (Table S2 in the Supporting Information) that targeted on *xiaD* (a hydroxymethylbutenyl pyrophosphate reductase encoding gene) (Figure 1). Four out of these six cosmid clones were also

positive with a pair of specific primers XiaN-1F and XiaN-1R (Table S2 and Figure S1 in the Supporting Information) that targeted on *xiaN* (a polyprenyl diphosphate synthase encoding gene).

Preliminary Determination of the *xia* Gene Cluster Boundaries. The *orf(-1)* gene is located upstream of *xiaA* and encodes a putative zinc dependent alcohol dehydrogenase. Given the high amino acid sequence identity (68%) of Orf(-1) to Ox4, a known enzyme involved in macrolactam HSAF (dihydromaltophilin) biosynthesis in *Lysobacter enzymogenes*,²² we exclude its role in XMA/OXM biosynthesis. In support of this prediction, the *orf(-1)*-inactivation mutant (Figure S2 in the Supporting Information) still produced XMA/OXM at a level comparable to that of the wild type strain (Figure 2, traces

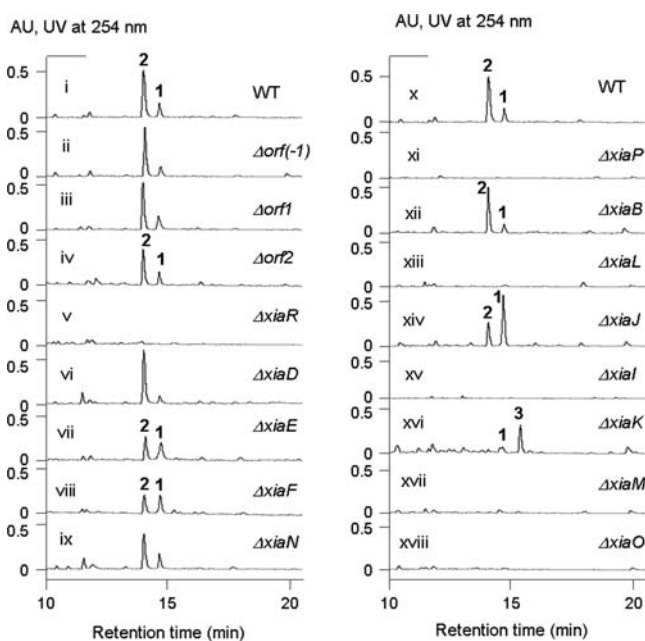


Figure 2. HPLC analysis of metabolite profile of the *xia* gene knockout mutants. (i) Wild type *Streptomyces* sp. SCSIO 02999; (ii) $\Delta orf(-1)$ mutant XM31; (iii) $\Delta orf1$ mutant XM50; (iv) $\Delta orf2$ mutant XM51; (v) $\Delta xiaR$ mutant XM49; (vi) $\Delta xiaD$ mutant XM35; (vii) $\Delta xiaE$ mutant XM36; (viii) $\Delta xiaF$ mutant XM37; (ix) $\Delta xiaN$ mutant XM45; (x) wild type *Streptomyces* sp. SCSIO 02999; (xi) $\Delta xiaP$ mutant XM47; (xii) $\Delta xiaB$ mutant XM33; (xiii) $\Delta xiaL$ mutant XM43; (xiv) $\Delta xiaJ$ mutant XM40; (xv) $\Delta xiaI$ mutant XM41; (xvi) $\Delta xiaK$ mutant XM42; (xvii) $\Delta xiaM$ mutant XM44; (xviii) $\Delta xiaO$ mutant XM46. The products XMA (1), OXM (2), and indosespene (3) are indicated.

i, ii). Unexpectedly, the construction of *xiaA*-inactivation mutant was futile after trying many times with the conventional lambda-RED-mediated gene replacement method. Thereby, we could not rule out the possibility that *xiaA* is related to XMA/OXM biosynthesis. Downstream of *xiaR*, there are two *orf*s (Figure 1). They encode proteins having predicted functions not relevant to XMA/OXM biosynthesis (Table 1); we hypothesize that they are beyond the *xia* gene cluster. To validate this hypothesis, we disrupted *orf1*, encoding a putative zinc metalloprotease, and *orf2*, encoding a putative sodium-coupled permease, by insertional mutation with an apramycin-resistant gene cassette (Figure S2 in the Supporting Information). The production of XMA/OXM was not affected in both $\Delta orf1$ and $\Delta orf2$ mutants (Figure 2, traces iii, iv),

clearly excluding their involvements in XMA/OXM biosynthesis. In contrast, the disruption of *xiaR*, a LuxR family transcriptional regulator, completely abolished XMA/OXM production (Figure 2, trace v), demonstrating its essentiality for XMA/OXM biosynthesis. Thus, we propose that 18 *orf*s, from *xiaA* to *xiaR*, are probably involved in XMA/OXM biosynthesis (Figure 1).

Genes Putatively Involved in Terpene Biosynthesis.

Five genes, *xiaDEFNP*, are probably involved in the formation of the XMA/OXM terpenoid skeleton. XiaD displays the highest similarity to the 4-hydroxy-3-methylbut-2-en-1-yl pyrophosphate (HMBPP) reductase (IspH) from *Kribbella flavida* DSM 17836. XiaE shows 63% identity to 1-deoxy-D-xylulose-5-phosphate (DXP) synthase (DXS) from *Catenulipora acidiphila* DSM 44928. XiaF exhibits 90% identity to an HMBPP synthase (IspG) from *Saccharopolyspora spinosa* NRRL 18395. These three enzymes are probably responsible for providing IPP and DMAPP via the non-mevalonate pathway.¹⁵ The non-mevalonate pathway was discovered in the late 1990s and was established to require seven consecutive steps involving the enzymes DXS, IspC (1-deoxy-D-xylulose 5-phosphate reductase), IspD (4-diphosphocytidyl-2-C-methyl-D-erythritol synthase), IspE (4-diphosphocytidyl-2-C-methyl-D-erythritol kinase), IspF (2-C-methyl-D-erythritol 2,4-cyclo-diphosphate synthase), IspG, and IspH in bacteria.^{15a,d,23}

However, only three genes in the *xia* cluster are identified to encode equivalent enzymes to this minipathway, namely *xiaE* (*dxs*), *xiaF* (*ispG*), and *xiaD* (*ispH*); the other four genes (*ispCDEF*) are missing in the *xia* cluster. Bioinformatic analyses of the not-yet-completed genome sequences of *Streptomyces* sp. SCSIO 02999 revealed the presence of several other gene copies with predicted functions similar to these seven proteins outside the *xia* cluster. In accordance with these findings, both XMA (1) and OXM (2) were still produced in the $\Delta xiaD$, $\Delta xiaE$, and $\Delta xiaF$ mutants (Figure 2, traces vi–viii), probably due to the cross-complementation of other gene copies with equivalent functions to XiaD, XiaE, and XiaF in the chromosome of *Streptomyces* sp. SCSIO 02999. It seemed that XMA/OXM productions were not affected in the $\Delta xiaD$ mutant (Figure 2, trace vi); however, the yields and ratios of XMA (1) to OXM (2) appeared to be changed upon knockout of *xiaE* and *xiaF* (Figure 2, traces vii, viii).

XiaN exhibits above 50% identity to a number of predicted polyprenyl diphosphate synthases, mostly from *Streptomyces* species, with the highest similarity to HopB from *Streptomyces avermitilis* MA-4680.²⁴ The overall similarity of XiaP to polyprenyl diphosphate synthases is below 40% identity, with the maximum homology (44% identity) to SSNG_07282, a predicted polyprenyl diphosphate synthase from a *Streptomyces* species. Both XiaN and XiaP contain two conserved aspartate-rich DDXXD motifs. The aspartates in these motifs are proposed to form binding pockets for the diphosphate moieties of the substrates (IPP or DMAPP) through Mg^{2+} bridges, which are supported by crystal structure studies on such enzymes.²⁵ Based on these bioinformatic analyses, both XiaN and XiaP are possibly involved in catalyzing the successive 1'–4 condensation of the 5-carbon IPP to allylic DMAPP to form farnesyl diphosphate (FPP), which is a key component in assembling XMA/OXM. However, our gene-inactivation experiments revealed that the $\Delta xiaN$ mutant preserved XMA/OXM production (Figure 2, trace ix), albeit with a slightly reduced yield. In contrast, the $\Delta xiaP$ mutant lost the XMA/OXM production (Figure 2, trace xi).

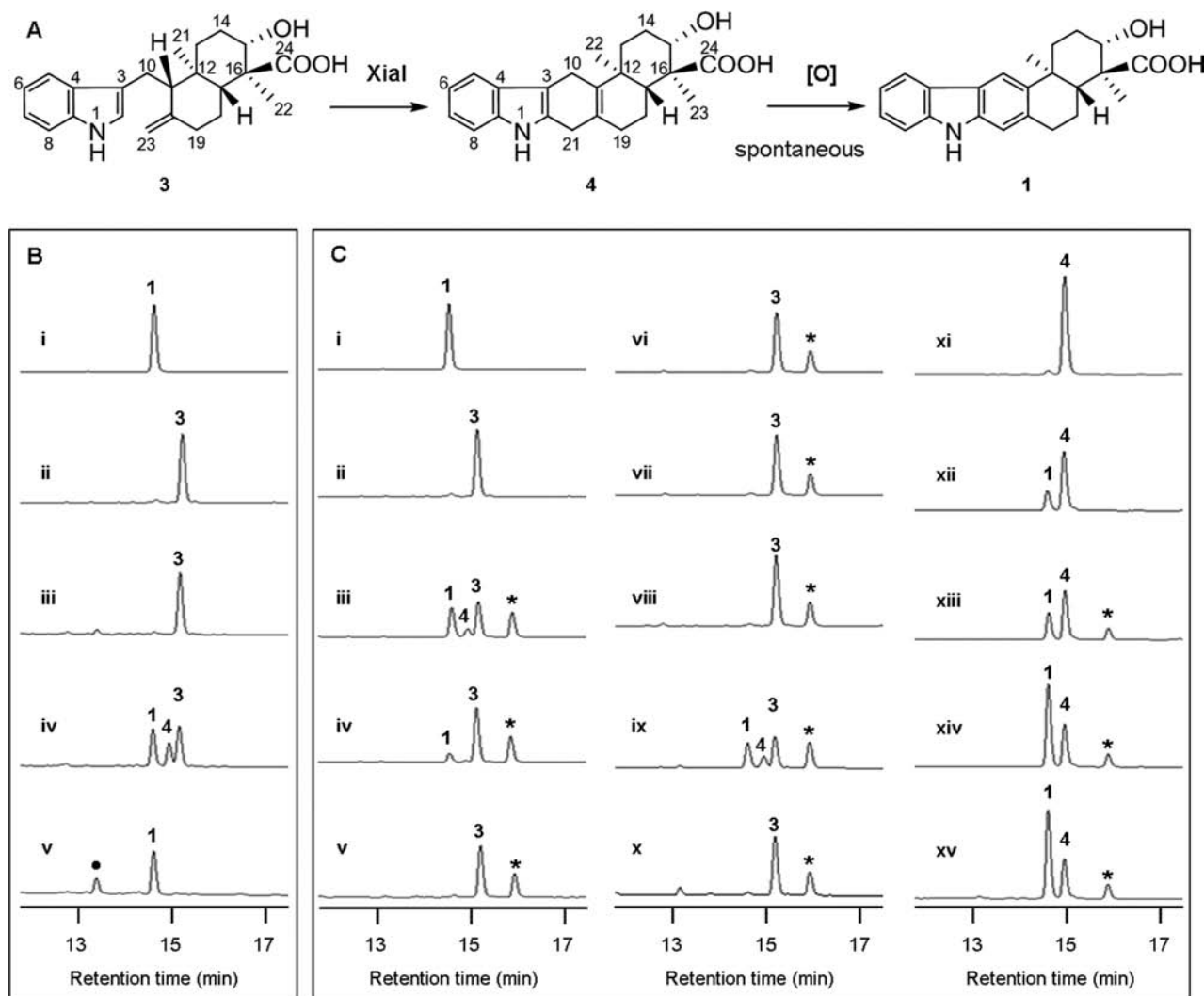


Figure 3. Biotransformation of indospesene (3) in *E. coli* and in vitro characterization of Xial-catalyzed reactions. (A) A scheme for Xial catalysis. (B) HPLC analysis of *E. coli*-mediated biotransformation of indospesene (3). (i) XMA (1) standard; (ii) indospesene (3) standard; (iii) control *E. coli* BL21(DE3)/pET28a supplemented with 30 μM indospesene (3) after 4 h; (iv) *E. coli* BL21(DE3)/pCSG2604 supplemented with 30 μM indospesene (3) after 4 h; (v) *E. coli* BL21(DE3)/pCSG2604 supplemented with 30 μM indospesene (3) after 24 h. (C) HPLC analysis of in vitro Xial assays. (i) XMA (1) standard; (ii) indospesene (3) standard; (iii) standard Xial assay comprising 400 μM 3, 1 mM FAD, 2 mM NADH, and 5 μM Xial in 50 mM Tris-HCl (pH 8.0) buffer, incubated at 28 $^{\circ}\text{C}$ for 4 h; (iv) standard Xial assay minus FAD; (v) control assay using boiled Xial; (vi) standard Xial assay minus NADH; (vii) standard Xial assay minus NADH; (viii) Xial assay comprising 400 μM 3, 1 mM FAD, and 2 mM NADH without Xial or boiled Xial; (ix) standard Xial assay in which 1 mM FAD was replaced by 1 mM FMN; (x) control assay comprising 400 μM 3, 1 mM FMN, 2 mM NADH, and boiled Xial; (xi) purified prexiamycin (4) before NMR analysis; (xii) purified prexiamycin (4) after NMR analysis; (xiii) 400 μM 4 was kept in 50 mM Tris-HCl (pH 8.0) buffer at 28 $^{\circ}\text{C}$ for 4 h; (xiv) 400 μM 4 was incubated with 1 mM FAD, 2 mM NAD, and 5 μM Xial in 50 mM Tris-HCl (pH 8.0) buffer at 28 $^{\circ}\text{C}$ for 4 h; (xv) 400 μM 4 was incubated with 1 mM FAD, 2 mM NAD, and boiled Xial in 50 mM Tris-HCl (pH 8.0) buffer at 28 $^{\circ}\text{C}$ for 4 h. The bullet (\bullet) denotes an unknown compound from *E. coli*; an asterisk (*) denotes an unknown impurity in Xial assays.

Genes Encoding Regulators and Transporters. Five regulator- or transporter-encoding genes *xiaCGHQR* are identified in the *xia* cluster. XiaC contains a helix-turn-helix motif [pfam09339] at the N-terminus and an IclR superfamily motif [pfam01614] at the C-terminus, with the highest similarity (35% identity) to Trd_0252, a predicted IclR family bacterial transcriptional regulator from *Thermomicrobium roseum* DSM 5159. XiaG displays the highest homology to Micau_3829, a LuxR regulatory protein from *Micromonospora aurantiaca* ATCC 27029. Both XiaQ and XiaR encode putative large ATP-binding regulators of the LuxR family (LAL) proteins. Members of the LAL family contain an ATP-binding domain at the N-terminus (Walker A and B motifs) and a helix-

turn-helix domain for DNA binding at the C-terminus,²⁶ and have been identified as pathway activators for several natural products.²⁷ In accordance with bioinformatics analysis, the $\Delta xiaR$ mutant abolished XMA/OXM production (Figure 2, trace v), indicating that it acted as a pathway activator. XiaH encodes a putative transporter with the highest similarity to a putative membrane protein (BAD07391) from *Actinoplanes* sp. A40644 (Table 1), putatively involved in XMA/OXM transportation or resistance.

Putative Oxidoreductase-Encoding Genes. Eight genes, *xiaABIJKLMO*, may encode oxidoreductases involved in XMA/OXM biosynthesis. The deduced product of *xiaA* contains an N-terminal Rieske [2Fe-2S] binding domain characteristic for

members of the Rieske non-heme iron oxygenase (RO) family, a large class of aromatic ring hydroxylating dioxygenases predominantly found in microorganisms.²⁸ ROs consist of two or three components, reductase, oxygenase, and ferredoxin, in which the Rieske [2Fe–2S] cluster accepts electrons from the reductase or ferredoxin component and transfers them to the mononuclear iron for catalysis. Interestingly, *xiaB* encodes an FMN-binding domain containing flavin reductase and *xiaL* is predicted to encode a ferredoxin (Table 1). Thus, XiaABL may constitute an RO family. XiaI exhibits overall sequence similarities to naphthocyclinone hydroxylase NcnH [cd01159] and acyl-CoA dehydrogenase ACAD [cd00567], with the highest identity being with an indole oxygenase from an uncultured bacterium JEC54.²⁹ XiaJ contains a limonene-1,2-epoxide hydrolase catalytic domain LEH [pfam07858]. Epoxide hydrolases usually catalyze the hydrolysis of epoxides to corresponding diols.³⁰ XiaK displays the highest sequence identity to an aromatic ring hydroxylase RHA1_ro00538 from *Rhodococcus jostii* RHA1, and contains an N-terminal FAD binding domain (pfam01494) and a central Rossmann-fold NAD(P)-binding domain. XiaM shows an overall higher than 45% sequence identity to a number of cytochrome P450s, including PtmO5 for diterpenoid platensimycin biosynthesis.³¹ XiaO is a rather large protein of 718 amino acids in size. It contains a tryptophan 2,3-dioxygenase domain [pfam03301] at the N-terminus and an FAD dependent oxidoreductase domain [pfam12831] at the C-terminus.

It is hard to assign functions to these eight putative oxidoreductases for XMA/OXM biosynthesis only by bioinformatic analyses. To gain insights into their roles in the XMA/OXM pathway, we then made gene-disruption mutants for these genes (Figure S2 in the Supporting Information). The $\Delta xiaB$ mutant still produced both XMA and OXM (Figure 2, trace xii), comparable to WT (Figure 2, trace x), indicating that the flavin reductase XiaB was not essential for XMA/OXM biosynthesis. Since several other flavin reductase-encoding genes were found in the genome sequence of SCSIO 02999 (data not shown), they likely complemented *xiaB* to maintain the biosynthesis of XMA/OXM. Notably, the $\Delta xiaJ$ mutant still produced both XMA and OXM (Figure 2, trace xiv); however, the production ratio of XMA to OXM was quite different from that of WT (Figure 2, trace x). The $\Delta xiaK$ mutant accumulated a new biosynthetic intermediate (Figure 2, trace xvi), which was isolated from a 15 L fermentation broth for structural analysis. The ¹H and ¹³C NMR spectral data of this isolated intermediate were identical to those reported for indosespene 3 (Figure S3 in the Supporting Information).^{13b} Thus, the intermediate was characterized to be indosespene (3). Unexpectedly, a minor amount of XMA (1) could still be isolated from the $\Delta xiaK$ mutant (Figure 2, trace xvi). However, no OXM (2) was detected in the $\Delta xiaK$ mutant (Figure 2, trace xvi). These data indicated that XiaK was not required for XMA (1) biosynthesis but was essential for OXM (2) production. Unfortunately, the other four mutants ($\Delta xiaL$, $\Delta xiaI$, $\Delta xiaM$, $\Delta xiaO$) were devoid of XMA/OXM productions and produced no detectable intermediates (Figure 2, traces xiii, xv, xvii, xviii).

Feeding XMA/OXM Nonproducing Mutants With Indosespene and XMA. Since most gene-knockout mutants produced no intermediates, our gene-inactivation experiments provided few clues for elucidating the XMA/OXM biosynthetic pathway. Only indosespene (3) was obtained as a putative biosynthetic intermediate from the $\Delta xiaK$ mutant. Subsequently, we fed indosespene (3) to five XMA/OXM non-

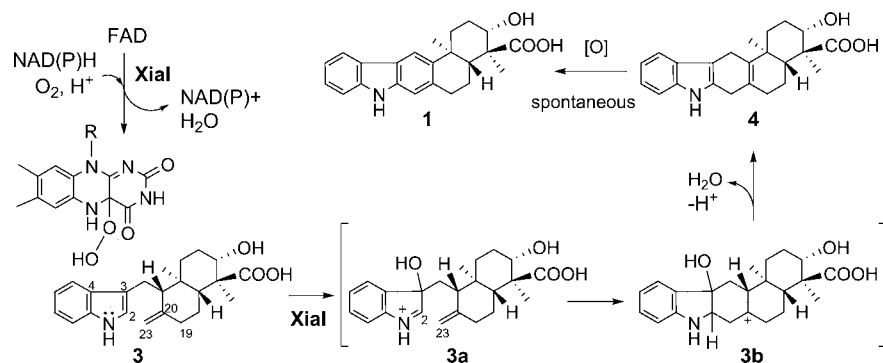
producing mutants ($\Delta xiaI$, $\Delta xiaL$, $\Delta xiaM$, $\Delta xiaO$, $\Delta xiaP$). Interestingly, upon feeding of indosespene (3), the $\Delta xiaL$, $\Delta xiaM$, and $\Delta xiaP$ mutants restored both XMA production and OXM production (Figure S4A–C in the Supporting Information), whereas the $\Delta xiaO$ mutant restored XMA production but not OXM production (Figure S4D in the Supporting Information), and no consumption of 3 occurred in the $\Delta xiaI$ mutant (Figure S4E in the Supporting Information). We also fed XMA (1) to four mutants ($\Delta xiaI$, $\Delta xiaM$, $\Delta xiaK$, and $\Delta xiaO$). XMA could be converted to OXM by the $\Delta xiaI$ and $\Delta xiaM$ mutants (Figure S4F,G in the Supporting Information), but remained unchanged in the $\Delta xiaK$ and $\Delta xiaO$ mutants (Figure S4H,I in the Supporting Information).

Identification of Xial as an Enzyme Catalyzing a Novel Cyclization Reaction. Given no further process of indosespene (3) in the $\Delta xiaI$ mutant, we hypothesized that indosespene (3) was an immediate substrate for XiaI. To validate this hypothesis, we first fed 3 to an *E. coli* BL21(DE3) strain harboring the plasmid pCSG2604 (Table S1 in the Supporting Information), in which the PCR-amplified, sequence-confirmed *xial* gene was inserted. After inducing *xial* expression with IPTG, indosespene (3) was converted to a new intermediate (4) and XMA (1) (Figure 3B, trace iv), and was completely converted to XMA (1) upon longer incubation (Figure 3B, trace v). As a control, *E. coli* BL21(DE3)/pET28a could not process indosespene (3) (Figure 3B, trace iii). The new intermediate 4 displayed a UV spectrum similar to that of 3, but different from that of XMA (1) (Figure S5 in the Supporting Information). Subsequently, this intermediate (4) was isolated from *E. coli* BL21(DE3)/pCSG2604 mediated large scale biotransformation of indosespene (3) and subjected to structural analysis.

The molecular formula of compound 4 was determined to be C₂₃H₂₇NO₃ on the basis of HRFABMS (*m/z* 366.2099 [M + H]⁺), indicating one more unsaturation degree than indosespene (3). ¹H and ¹³C NMR spectral data of 4 revealed the presence of two singlet methyls ($\delta_{\text{H}}/\delta_{\text{C}}$ 1.13/20.7, 1.18/11.4) six sp³ methylenes, including two with relatively downfield proton shifts ($\delta_{\text{H}}/\delta_{\text{C}}$ 3.17, 3.22/30.7; 3.34/22.6), two sp³ methines (one was oxygenated), four sp² methines, two sp³ hybridized quaternary carbons and six sp² hybridized quaternary carbons, and a carbonyl carbon (δ_{C} 182.0) (Table S3 and Figure S6 in the Supporting Information). In a comparison of the ¹H and ¹³C NMR spectral data of 4 and 3, the singlet olefinic proton (δ_{H} 6.89, H-2) and the two terminal double bond protons (δ_{H} 4.80, 4.71, H-23) in 3 were missing in 4. Considering one more degree of unsaturation of 4 than 3, it implied that C-2 and C-23 in 3 were connected to form a ring in 4, which was supported by the key HMBC correlations from H-21 to C-3/C-11/C-19 in 4 (Figures S6 and S7 in the Supporting Information). Simultaneously, the double bond between C-20 and C-23 in 3 was shifted between C-11 and C-20 in 4. In support of this shift, one more sp³ methylene ($\delta_{\text{H}}/\delta_{\text{C}}$ 3.17, 3.22/30.7, C-21) was observed in 4, and the methine ($\delta_{\text{H}}/\delta_{\text{C}}$ 2.27/57.8, C-11) in 3 was substituted by a quaternary carbon (δ_{C} 137.1) in 4. This double bond shift was further confirmed by HMBC correlations from H-10 to C-2/C-20 and from H₃-22 to C-11/C-12/C-13/C-17 (Figures S6 and S7 in the Supporting Information). Thus, the structure of 4 was determined as shown in Figure 3A, named “prexiamycin”.

Next, N-His₆-tagged XiaI was purified to near homogeneity (Figure S8 in the Supporting Information). In an in vitro assay comprising 400 μM indosespene (3), 1 mM FAD, 2 mM

Scheme 2. Proposed XiaI Reaction Mechanism



NADH, and 5 μM Xial, in 50 mM Tris-HCl buffer (pH 8.0), indospesene (**3**) was indeed converted to XMA (**1**), via the intermediate prexiamycin (**4**) (Figure 3C, traces i–iii). Xial could also use NADPH as a cofactor, however, at an apparently lower consumption ratio of **3** than NADH under the same assay conditions (Figure 3C, traces iii, iv). In a control assay with boiled Xial (Figure 3C, trace v), and in other control assays lacking either FAD (Figure 3C, trace vi), NAD(P)H (Figure 3C, trace vii), or enzymes (Xial or boiled Xial) (Figure 3C, trace viii), no conversions of indospesene (**3**) were observed. When FAD was replaced by FMN in Xial assays, indospesene (**3**) could also be converted to **1–4** (Figure 3C, trace ix), and no conversion of indospesene (**3**) was observed in the control assay with FMN, NADH, and boiled Xial (Figure 3C, trace x). These experiments confirmed that Xial catalyzed a flavin dependent oxidative cyclization reaction.

It should be noted that we observed a spontaneous conversion of prexiamycin (**4**) to XMA (**1**) during the structural characterization of prexiamycin (**4**). The purified prexiamycin (**4**) (Figure 3C, trace xi) was quickly and partially converted to **1** (Figure 3C, trace xii) during recording of NMR data. This problem was resolved by reisolating **4**, removing air from the solution of **4** by nitrogen, and performing immediate NMR analysis. This phenomenon indicated that the conversion of **4** to **1** was probably a nonenzymatic, spontaneously oxidative process. Next, we checked if Xial could promote the conversion of prexiamycin (**4**) to XMA (**1**). In an *in vitro* assay comprising 400 μM prexiamycin (**4**), 1 mM FAD, 2 mM NAD, and 5 μM Xial, in 50 mM Tris-HCl buffer (pH 8.0), the conversion ratio of prexiamycin (**4**) to XMA (**1**) was comparable to that of the corresponding control assay with boiled Xial (Figure 3C, traces xiv, xv). Interestingly, a lower conversion ratio of **4** to **1** was observed in the control assay containing only 50 mM Tris-HCl (pH 8.0) buffer without FAD, NAD, and Xial (or boiled Xial) (Figure 3C, trace xiii).

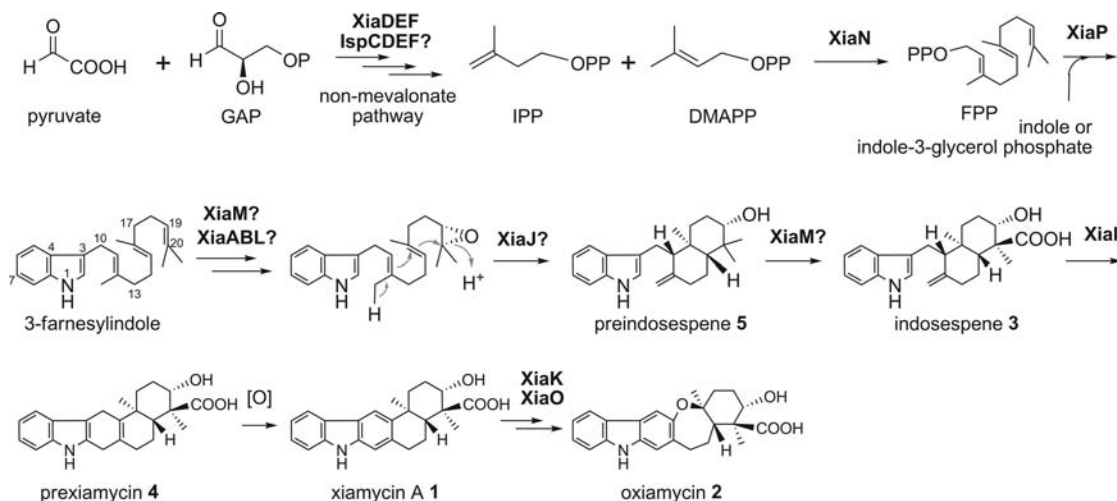
DISCUSSION

By partial genome sequencing, we have identified a single *xia* gene cluster responsible for biosynthesizing both XMA and OXM, two indolosesquiterpene natural products produced by the marine-derived *Streptomyces* sp. SCSIO 02999. The presence of *xiaD*, *xiaE*, and *xiaF* in the *xia* gene cluster, functionally equivalent to *ispH*, *dxs*, and *ispG*, respectively, clearly demonstrates that the isoprene building blocks for constructing the terpenoid portion of XMA/OXM are derived from the non-mevalonate pathway. However, the other four genes (*IspCDEF*) involved in the non-mevalonate pathway are absent from the *xia* gene cluster. Consistent with that all

actinomycetes are equipped with the non-mevalonate pathway for isoprene production during primary metabolism,³² several copies of *ispCDEF*, as well as *dxs*, *ispG*, and *ispH*, are found dispersely distributed in the chromosome of *Streptomyces* sp. SCSIO 02999 outside the *xia* gene cluster. The first example of non-mevalonate pathway genes associated with secondary metabolism is the embedding of two genes *plaT5* (*ispG*) and *plaT6* (*dxs*) in the terpene phenalinolactone biosynthetic gene cluster, which are suggested to potentially enhance the isoprene production.^{32b} In support of this suggestion, the yields of XMA/OXM were slightly reduced in the $\Delta xiaE$ (*dxs*) and $\Delta xiaF$ (*ispG*) mutants (Figure 2, traces vii, viii).

Although bioinformatic analysis suggests that both *xiaN* and *xiaP* encode polyprenyl diphosphate synthases, the $\Delta xiaN$ mutant preserved XMA/OXM production while the $\Delta xiaP$ mutant lost the ability to produce XMA/OXM (Figure 2, traces ix, xi). These data indicated that XiaN and XiaP possessed distinct biosynthetic functions. We propose that XiaN could function as a farnesyl diphosphate (FPP) synthase. Since several other copies of polyprenyl diphosphate synthase genes are found outside the *xia* gene cluster in the SCSIO 02999 genome (data not shown), they may compensate for XiaN function in the $\Delta xiaN$ mutant, to maintain the supply of FPP. However, our current data could not ascribe an exact role for XiaP in XMA/OXM biosynthesis. We propose that XiaP might act as a prenyltransferase to install FPP to indole, providing 3-farnesylindole. A similar function was recently demonstrated for AuaA, a farnesyltransferase that catalyzes the direct linkage of FPP to 2-methyl-4-hydroxyquinoline in the biosynthesis of aurachins.³³ Alternatively, XiaP might use another FPP acceptor, indole-3-glycerol phosphate, which is proposed as a building block leading to the fungal synthesis of the indole diterpene, paxilline.³⁴

The presence of eight oxidoreductase-encoding genes in the *xia* gene cluster suggested a complicated oxidative/reductive pathway leading to the pentacyclic ring system of XMA/OXM. Unfortunately, most gene-knockout mutants lost the ability to produce XMA/OXM or any intermediates, probably due to polar effects caused by insertional mutations. Only the $\Delta xiaK$ mutant produced a biosynthetic intermediate indospesene (**3**). Fortunately, the feeding of indospesene (**3**) into other XMA/OXM nonproducing mutants chemically rescued XMA (**1**) and/or OXM (**2**) production and the outcome provided precious information on XMA/OXM biosynthesis: (i) upon feeding of indospesene (**3**), both $\Delta xiaM$ and $\Delta xiaP$ mutants restored XMA/OXM production, indicating that XiaP- and XiaM-catalyzed reactions should occur before indospesene formation; (ii) both XMA production and OXM production

Scheme 3. Proposed Biosynthetic Pathway for XMA (1) and OXM (2)^a

^aGAP, D-glyceraldehyde 3-phosphate; IPP, isopentenyl diphosphate; DMAPP, dimethylallyl diphosphate; FPP, farnesyl pyrophosphate.

were restored in the $\Delta xiaL$ mutant by feeding of indosespene, indicating that *xiaL*-encoded ferredoxin was involved in reactions before indosespene formation; (iii) the nonconsumption of indosespene in the $\Delta xiaI$ mutant indicated that the oxygenase XiaI-catalyzed reactions should occur after indosespene formation and XiaI was essential for both XMA and OXM biosynthesis; (iv) the $\Delta xiaK$ mutant could still produce a trace amount of XMA (1) but no OXM (2), demonstrating that XiaK was nonessential for XMA production but was required for OXM biosynthesis; (v) the $\Delta xiaO$ mutant could convert indosespene to XMA (1) but not to OXM (2), indicating that XiaO was only essential for OXM (2) production; (vi) cumulatively, these data proved indosespene as a common precursor en route to both XMA (1) and OXM (2) biosynthesis. Furthermore, the biotransformation of XMA to OXM in the $\Delta xiaI$ and $\Delta xiaM$ mutants indicated that XMA was a precursor to OXM. No conversions of XMA to OXM by the $\Delta xiaK$ and $\Delta xiaO$ mutants further confirmed that both enzymes were crucial to OXM biosynthesis.

The demonstration of XiaI as an enzyme driving the cyclization of indosespene (3) to produce XMA (1) and its identification as a single-component flavin dependent monooxygenase indicate that XiaI probably acts on the indole side chain of indosespene. We propose a mechanism that involves hydroxylation at C-3 of the indole moiety using a C-4a-hydroperoxy-FAD as the electrophilic oxygenating species (Scheme 2), similar to flavoprotein Af12060- and TqaH-catalyzed hydroxylations of the indole moiety in fumiquinazoline F.³⁵ The hydroxylation at C-3 of indosespene by XiaI likely requires the participation of the pyrrole NH group to form an indole C-3-hydroxyiminium species (3a), where an adjacent C-2 carbanion equivalent could be generated and be attacked by the neighboring C-23 olefin function in 3, thereby leading to a cyclization reaction to form 3b. Subsequently, the dehydration of 3b and the loss of a proton would afford prexiamycin (4). In support of this proposed mechanism, prexiamycin was isolated as a XiaI enzymatic reaction intermediate/product. Subsequently, prexiamycin (4) could undergo a nonenzymatic, spontaneous oxidative aromatization to form XMA (Scheme 2).

Several examples of the oxidation of the pyrrole ring of indoles by non-heme iron or cytochrome-type oxygenases have been reported. The XiaI closest homologue, an indole

oxygenase from an uncultured bacterium JEC54, was shown to confer heterologous production of indirubin and indigo in *E. coli*, putatively resulting from hydroxylation of indole,²⁹ in a mechanism analogous to an engineered variant of the flavoprotein 2-hydroxybiphenyl 3-monooxygenase HbpA,³⁶ whose in vitro enzymatic products by hydroxylation at indole C-2 or C-3 were unstable and spontaneously oxidized and dimerized to form indirubin and indigo.³⁶ Indole oxygenations were also found in the biosynthetic pathway for more complex natural products. The flavin dependent oxygenase VioC has been characterized for the oxidation at C-2 of a bisindole-pyrrolidone in the biosynthesis of violacein.³⁷ The C-3' hydroxylations of indole moiety in fumiquinazoline F by Af12060 and TqaH were shown to trigger a tandem oxidative-acylation strategy for the generation of multicyclic scaffolds in fungal indole alkaloid biosyntheses of fumiquinazoline A and tryptoqualanine.³⁵ The flavoprotein NotB was recently characterized in vitro to catalyze the indole 2,3-oxidation of notoamide E, leading to notoamides C and D via an apparent pinacol-like rearrangement in the biosynthesis of notoamide indole alkaloids.³⁸ Distinct from these reported indole oxygenases, XiaI-mediated oxygenation of indosespene (3), which eventually led to the formation of XMA (1) via prexiamycin (4), implicated a novel cyclization strategy tailoring indolosesquiterpene biosynthesis. The detailed mechanism of this novel enzymatic reaction is still under investigation.

Based on bioinformatics and our current experimental data, we proposed a putative biosynthetic pathway for XMA/OXM in marine-derived *Streptomyces* sp. SCSIO 02999 (Scheme 3). Biosynthesis of the terpenoid portion of XMA/OXM was initiated from pyruvate and D-glyceraldehyde 3-phosphate (GAP) by a non-mevalonate pathway to provide the requisite five-carbon building blocks IPP and DMAPP, involving XiaDEF and putative enzymes outside the *xia* gene cluster. The formation of FPP from IPP and DMAPP was probably catalyzed by XiaN, a predicted polyprenyl diphosphate synthase. Next, the prenyltransferase XiaP-catalyzed coupling of FPP with indole (or indole-3-glycerol phosphate) would lead to 3-farnesylindole. Since none of the genes in the *xia* cluster appeared to encode a terpene cyclase, which was commonly found in bacterial sesquiterpene biosynthesis,¹¹ we speculated

an intermolecular cyclization involving a 19,20-epoxidation and a subsequent hydrolysis-triggered cyclization to transform 3-farnesylindole to preindosespene (5, Scheme 3). Such chemistry was precedent in the fungal synthesis of indole diterpene paxilline and meroterpenoid pyripyropene.^{34,39} In pyripyropene biosynthesis, the FAD dependent monooxygenase Pyr5 was characterized in vivo to catalyze the epoxidation of the terminal alkene of the farnesyl moiety and a novel membrane-bound cyclase Pyr4 was revealed in vitro to catalyze the subsequent cationic cyclization.³⁹ Similarly in paxilline biosynthesis, the FAD dependent monooxygenase PaxM and the prenyltransferase PaxC were proposed to catalyze epoxidation and cyclization, respectively.³⁴ In the *xia* cluster, the cytochrome P450 XiaM could serve as an epoxidase, functionally equivalent to PaxM and Pyr5. The putative limonene-1,2-epoxide hydrolase XiaJ could catalyze the hydrolysis of the epoxide to trigger cyclization to form preindosespene (5). However, no intermediates were observed in the $\Delta xiaM$ mutant and both XMA (1) and OXM (2) were still produced in the $\Delta xiaJ$ mutant, making uncertain their roles in XMA/OXM biosynthesis. Since the ferredoxin XiaL was suggested from the feeding experiments to be involved in reactions prior to indosespene (3) formation, the putative RO family enzymes XiaABL could putatively participate in transforming 3-farnesylindole to preindosespene (5). The cytochrome P450 XiaM could alternatively catalyze the oxidation of one of the C-24 methyl groups in preindosespene (5) to form the carbonyl group in indosespene, in analogy to NysN and AmphN, two cytochrome P450s providing the exocyclic carboxyl groups in the polyene antibiotics nystatin and amphotericin B.⁴⁰ Subsequently, the indole oxygenase XiaI was confirmed to catalyze the conversion of indosespene (3) to prexiamycin (4), which underwent spontaneous oxidation to form XMA (1). However, our current data gave no clues on the possible ways finalizing OXM formation, which required the insertion of an oxygen atom between C-11 and C-13. Such an unusual chemistry might involve XiaO, a probable bifunctional protein containing an N-terminal tryptophan 2,3-dioxygenase domain and a C-terminal FAD dependent oxidoreductase domain. Nevertheless, our biotransformation experimental data indicated that XMA was a precursor of OXM and two enzymes, XiaK and XiaO, were pivotal in the transformation of XMA (1) to OXM (2). The detailed biosynthetic steps leading to OXM are currently under investigation.

In conclusion, we identified and characterized the *xia* gene cluster for XMA/OXM biosynthesis in marine-derived *Streptomyces* sp. SCSIO 02999. Inactivation of 13 *xia* genes and analysis of metabolite profiles of the resulting mutants confirmed the identity of the *xia* gene cluster. Feeding of a biosynthetic intermediate indosespene into nonproducing mutants revealed indosespene as a precursor common to XMA/OXM biosynthesis and demonstrated the timing for enzymes involved in oxidative/reductive reactions. Most notably, functional elucidation of the indole oxygenase XiaI revealed a novel cyclization strategy for indolosesquiterpene biosynthesis.

EXPERIMENTAL SECTION

Bacterial Strains, Plasmids, and Reagents. Strains and plasmids used and generated in this study are listed in Table S1 in the Supporting Information. *Streptomyces* sp. SCSIO 02999 was isolated from the sediment of the South China Sea (E 109°153.171', N 116°103.576') at a depth of 880 m. Chemicals and reagents for

biochemical and molecular biology were purchased from standard commercial sources.

DNA Manipulation, Sequencing, and Bioinformatic Analysis.

DNA manipulations in *E. coli* and actinomycetes were performed according to standard procedures.⁴¹ PCR amplifications were carried out on an Authorized Thermal Cycler (Eppendorf AG). Primers were synthesized at Sangon Biotech (Shanghai) Co. Ltd. The 454 shotgun partial genomic sequencing of *Streptomyces* sp. SCSIO 02999 was carried out at the Chinese National Genome Center (Shanghai), and common DNA sequencing was performed at Invitrogen Biotech Co., Ltd. (Guangzhou). The DNA sequence of the *xia* gene cluster has been deposited into GenBank under the accession number JQ812811. The orf's were determined by use of the FramePlot 4.0beta program (<http://nocardia.nih.gov/jp/fp4/>). Protein sequences were compared with the BLAST program (<http://blast.ncbi.nlm.nih.gov/Blast.cgi>).

Genomic Library Construction and Screening. A genomic library of *Streptomyces* sp. SCSIO 02999 was constructed in SuperCos1 by using the MaxPlax Lambda Packaging Extract system according to the manufacturer's instructions (Epicenter, Madison, WI, USA). Two pairs of specific primers were designed to target on either *xiaD* (XiaD-1F, 5'-CGTCGAGCGGGCGCTGGAATC-3'; XiaD-1R, 5'-TCAGC-CACGTCACCACCTCCG-3') or *xiaN* (XiaN-1F, 5'-CGCAGAT-GAACAGGATCGCC-3'; XiaN-1R, 5'-ATCTGCCGGTCCGCT-CGTTCT-3') and were used to screen against approximately 2400 colonies by PCR.

Gene Inactivation Experiments. The lambda-RED-mediated gene replacements were performed as standard procedures.⁴² Detailed procedures for individual *xia* gene inactivation are described in Figure S2 in the Supporting Information.

Production, Isolation, and Structural Elucidation of XMA and Its Analogues.

The wild type strain *Streptomyces* sp. SCSIO 02999 and the mutants were cultured in modified 38# medium (malt extract 0.5%, yeast extract 0.4%, glucose 0.4%, vitamins 1%, sea salt 3%, pH 7.0–7.2) or modified ISP4 medium (soluble starch 1%, bacterial peptone 0.1%, yeast extract 0.05%, (NH₄)₂SO₄ 0.2%, CaCO₃ 0.2%, K₂HPO₄ 0.1%, MgSO₄·7H₂O 0.1%, NaCl 0.1%, FeSO₄·7H₂O 0.0001%, MnCl₂·6H₂O 0.0001%, ZnSO₄·7H₂O 0.0001%, sea salt 3%, pH 7.0) for 3–5 days. The 5% inoculums were seeded in 200 mL of production medium AM6 (soluble starch 2%, glucose 1%, bacterial peptone 0.5%, yeast extract 0.5%, CaCO₃ 0.5%, sea salt 3%, pH 7.0) in 1 L flask and then shaken at 220 rpm and 28 °C for 6–8 days. The production of XMA and its analogues was monitored via HPLC analysis on a Varian Star Workstation. HPLC was carried out using a reversed phase column Luna C18, 5 μm, 150 × 4.6 mm (Phenomenex), with UV detection at 254 nm under the following program: solvent system (solvent A, 10% acetonitrile in water supplementing with 0.1% formic acid; solvent B, 90% acetonitrile in water); 5% B to 100% B (linear gradient, 0–20 min), 100% B (20–21 min), 100% B to 5%B (21–22 min), 5% B (22–30 min); flow rate 1 mL/min.

For isolation of products from the $\Delta xiaK$ mutant, a total of 15 L of culture was prepared for fermentation. The 15 L fermentation cultures were separated to supernatant and mycelium cakes by centrifugation. The supernatants were absorbed by XAD-16 resin, and then the resin was eluted with 6 L of acetone; the mycelium cakes were extracted 4 times with 6 L of methanol. After removal of the organic solvents by evaporation, the two extracts were mixed and re-extracted with 6 L of butanone to afford 8.58 g of crude extracts after evaporation of organic solvents under vacuum. The crude extracts were subjected to a silica gel column (100–200 mesh, 7.5 g) and eluted with CHCl₃/CH₃OH (100/0, 100/1, 100/2, 100/4, 100/8, 100/16, 100/32, and 0/100, v/v, each of 450 mL) to yield eight fractions (Fr.1 to Fr.8). Fr.4 and Fr.5 were combined and subjected to MPLC (medium pressure liquid chromatography, YMC*GEL ODS-A, 12 nm, S-50 μm), eluted with CH₃OH/H₂O gradient to give the subfractions Fr.5-1 to Fr.5-10. Compound 3 (90.4 mg) was obtained as a gray powder from Fr.5-9. Indosespene (3): gray powder, ESI-MS *m/z* 368.4 [M + H]⁺, 390.5 [M + Na]⁺, 366.1 [M – H][–]; ¹H NMR (500 MHz, CD₃OD) δ_H: 7.53 (1H, d, *J* = 8.0, H-5), 7.28 (1H, d, *J* = 8.0, H-8), 7.04 (1H, t, *J* = 7.5, H-7), 6.98 (1H, t, *J* = 7.3, H-6), 6.89 (1H, s, H-2), 4.80 (1H, s, H-23a),

4.73 (1H, s, H-23b), 4.06 (1H, dd, $J = 10.5, 5.0$, H-15), 2.97 (1H, d, $J = 15.0, H-10a$), 2.83 (1H, dd, $J = 15.0, 10.5$, H-10b), 2.34 (1H, d, $J = 11.5, H-19a$), 2.27 (1H, d, $J = 10.0, H-11$), 2.08 (1H, d, $J = 13.5, H-13a$), 1.99 (1H, m, H-19b), 1.95 (1H, m, H-17), 1.75 (1H, m, H-14a), 1.70 (1H, m, H-14b), 1.58 (1H, m, H-18a), 1.50 (1H, m, H-13b), 1.32 (1H, m, H-18b), 1.11 (3H, s, H-21), 0.88 (3H, s, H-22); ^{13}C NMR (125 MHz, CD_3OD) δ_{C} : 11.6 (CH_3 , C-22), 15.3 (CH_3 , C-21), 20.9 (CH_2 , C-10), 27.6 (CH_2 , C-18), 28.5 (CH_2 , C-14), 38.6 (CH_2 , C-13), 39.0 (CH_2 , C-19), 40.2 (C, C-12), 52.1 (C, C-17), 55.1 (CH_3 , C-16), 58.0 (CH, C-11), 76.6 (CH, C-15), 109.0 (CH_2 , C-23), 112.2 (CH, C-8), 115.8 (C, C-4), 119.3 (CH, C-5), 119.4 (CH, C-6), 122.1 (CH, C-7), 123.4 (CH, C-2), 129.2 (C, C-3), 138.0 (C, C-9), 149.1 (C, C-20), 181.6 (C, C-24).

Feeding Experiments With Indosespene and XMA. The five XMA/OXM nonproducing mutants ($\Delta xiaI$, $\Delta xiaL$, $\Delta xiaM$, $\Delta xiaO$, and $\Delta xiaP$) were individually inoculated into 2 mL of AM6 medium supplemented with 30 μM indosespene (3). After incubation at 28 °C for 7 days, the cultures were extracted with 3 mL of butanone and were subjected to HPLC analysis. Four mutants ($\Delta xiaI$, $\Delta xiaL$, $\Delta xiaM$, and $\Delta xiaO$) were fed with 30 μM XMA (1) and were treated for HPLC analysis in the same way as for indosespene feedings.

Heterologous Production and Purification of Xial. The *xial* gene was PCR amplified from genomic DNA of *Streptomyces* sp. SCSIO 02999 using the following primer pair: 5'-AGTGGTGCA-TATGACAGACATCCGA-3' (*XiaI*-3F, *NdeI*) and 5'-AGGGGAG-GATCCGAAAGGAGGGT-3' (*XiaI*-3R, *BamHI*) with high fidelity DNA polymerase Pyrobest (Takara). PCR products were digested with *NdeI/BamHI* and inserted into the vector pET28a to give the expression plasmid pCSG2604 after sequence confirmation (Table S1 in the Supporting Information). The strain *E. coli* BL21(DE3) carrying pCSG2604 was grown in LB medium containing kanamycin at 37 °C to an A_{600} of around 0.7, and the expression of Xial was then induced by the addition of 0.1 mM isopropyl- β -D-thiogalactopyranoside (IPTG) for 8–10 h at 16 °C. *N*-(His)₆-tagged Xial proteins were then purified via nickel affinity chromatography. Cells were disrupted by sonification on ice after washing and resuspending with the lysing buffer (50 mM Tris-HCl, pH 8.0). The cellular lysates were centrifuged at 13500g for 0.5 h. The proteins were further purified by nickel-nitrilotriacetic acid (Ni^{2+} -NTA) agarose (Invitrogen) according to the manufacturer's protocols. The purified protein was desalted through a PD-10 column (GE Healthcare) and was concentrated by a Vivaspin concentrator (10 kDa, Sartorius). The protein concentration was determined by the Bradford method.⁴³ Purified *N*-(His)₆-tagged Xial was aliquoted and stored in 50 mM phosphate buffer (pH 7.4) containing 1 mM dithiothreitol (DTT) and 20% glycerol at -80 °C until use.

***E. coli* Mediated Biotransformation of Indosespene to Prexiamycin and XMA.** A single transformant of the strain *E. coli* BL21(DE3)/pCSG2604 was inoculated into 2 mL of LB containing 50 $\mu\text{g}/\text{mL}$ kanamycin and was grown to an A_{600} of around 0.7. Then, 0.1 mM IPTG and 30 μM indosespene (3) were added into the medium and grown at 28 °C for another 4 h. The products were extracted by butanone and were monitored by the above-mentioned HPLC program. To isolate the intermediate (4), a 500 mL culture of *E. coli* BL21(DE3)/pCSG2604 was made with supplementation of 200 μM indosespene (3) (about 36 mg in total). Then the culture was extracted by 1.5 L of butanone. After removal of the organic solvents under vacuum, 1.42 g of crude extracts was obtained. The crude extracts were subjected to a silica gel column (100–200 mesh, 1.5 g) and eluted with $\text{CHCl}_3/\text{CH}_3\text{OH}$ (100/0, 100/1, 100/2, 100/4, 100/8, 100/16, 100/32, and 0/100, v/v, each of 30 mL) to yield eight fractions (Fr.1 to Fr.8). Fractions Fr.2 to Fr.7 were combined and purified by semipreparative HPLC on a HITACHI D-2000 workstation, using a reversed phase column (C18, YMC*GEL ODS-A, 120A S-5 μm , 250 \times 10 mm; solvent A, 0.1% formic acid in water; solvent B, 90% acetonitrile in water; 55% constant gradient; flow rate 2.5 mL/min) to obtain compound 4 (7.0 mg). Compound 4 (7.0 mg) was immediately subjected to NMR analysis after dissolving in 600 μL of $\text{CD}_3\text{OD}/\text{CDCl}_3$ (4:1) and degassing with nitrogen. Prexiamycin (4) δ_{H} : 7.39 (1H, d, $J = 7.5, H-5$), 7.26 (1H, d, $J = 7.8, H-8$), 7.03 (1H,

t, $J = 7.8, H-7$), 6.97 (1H, t, $J = 7.5, H-6$), 4.05 (1H, dd, $J = 10.5, 4.5, H-15$), 3.34 (1H, m, H-10), 3.22 (1H, t, $J = 6.3, H-21a$), 3.17 (1H, t, $J = 5.8, H-21b$), 2.21 (1H, m, H-19a), 2.13 (1H, dd, $J = 16.5, 5.0, H-19b$), 2.10 (1H, m, H-17), 2.03 (1H, m, H-13a), 1.86 (1H, m, H-18a), 1.80 (2H, m, H-14), 1.53 (1H, m, H-13b), 1.45 (1H, m, H-18b), 1.18 (3H, s, H-23), 1.13 (3H, s, H-22); δ_{C} : 11.4 (CH_3 , C-23), 20.7 (CH_3 , C-22), 22.0 (CH_2 , C-18), 22.6 (CH_2 , C-10), 28.1 (CH_2 , C-14), 30.7 (CH_2 , C-21), 33.1 (CH_2 , C-19), 36.4 (CH_2 , C-13), 38.2 (C, C-12), 48.1 (CH, C-17), 54.5 (CH, C-16), 75.0 (CH, C-15), 107.6 (C, C-3), 111.6 (CH, C-8), 118.3 (CH, C-5), 119.4 (CH, C-6), 121.5 (CH, C-7), 124.6 (C, C-2), 128.3 (C, C-4), 132.5 (C, C-20), 137.8 (C, C-9), 137.1 (C, C-11), 182.0 (C, C-24).

Xial Enzyme Assays. A standard Xial assay contained 400 μM 3, 1 mM FAD (or FMN), 2 mM NADH (or NADPH), and 5 μM Xial in 50 mM Tris-HCl (pH 8.0) in a total volume of 100 μL . The reaction was performed at 28 °C for 2–24 h. Then assay mixtures were extracted with 3 volumes of ethyl acetate. After removal of ethyl acetate by vacuum evaporation, the residues were dissolved in methanol and subjected to HPLC analysis. The assays lacking FAD (or FMN) or NADH (or NADPH), or using boiled Xial (10 min at 100 °C), were carried out as controls. In assays with prexiamycin (4), the only difference was that NAD was used instead of NADH (or NADPH).

■ ASSOCIATED CONTENT

Supporting Information

Text for supplemental methods; Table S1, list of strains, plasmids; Table S2, list of primers; Figure S1, mapping and overlaps of selected positive cosmids; Figure S2, construction of mutants; Tables S3 and Figures S3, S5, S6, and S7, spectral data for compound characterization; Figure S4, biotransformation experiments; Figure S8, SDS-PAGE analysis of purified proteins. This material is available free of charge via the Internet at <http://pubs.acs.org>.

■ AUTHOR INFORMATION

Corresponding Author

czhang2006@gmail.com

Author Contributions

[§]These authors contributed equally to this work.

Notes

The authors declare no competing financial interest.

■ ACKNOWLEDGMENTS

This study was supported in part by the Funds of the 973 program (2010CB833805), the National Science Foundation of China (31125001), and the Chinese Academy of Sciences for Key Topics in Innovation Engineering (KZCX2-YW-JC202, KSCX2-EW-G-12). C.Z. is a scholar of the "100 Talents Project" of the Chinese Academy of Sciences (08SL111002). We are grateful for analytical facilities in the South China Sea Institute of Oceanology. We appreciate Profs. Shuangjun Lin (Shanghai Jiao Tong University, China) and Yuemao Shen (Shandong University, China) for helpful discussions.

■ REFERENCES

- (1) Leboeuf, M.; Hamonniere, M.; Cave, A.; Gottlieb, H. E.; Kunesch, N.; Wenkert, E. *Tetrahedron Lett.* **1976**, *17*, 3559.
- (2) Hocquemiller, R.; Dubois, G.; Leboeuf, M.; Cave, A.; Kunesch, N.; Riche, C.; Chiaroni, A. *Tetrahedron Lett.* **1981**, *22*, 5057.
- (3) Okorie, D. A. *Phytochemistry* **1981**, *20*, 2575.
- (4) Hasan, C. M.; Healey, T. M.; Waterman, P. G.; Schwalbe, C. H. J. *Chem. Soc., Perkin Trans. 1* **1982**, 2807.
- (5) Kunesch, N.; Cave, A.; Leboeuf, M.; Hocquemiller, R.; Dubois, G.; Guittet, E.; Lallemand, J. Y. *Tetrahedron Lett.* **1985**, *26*, 4937.

- (6) Nkonya, M. H. H.; Weenen, H. *Phytochemistry* **1989**, *28*, 2217.
- (7) Yoo, H. D.; Cremin, P. A.; Zeng, L.; Garo, E.; Williams, C. T.; Lee, C. M.; Goering, M. G.; O'Neil-Johnson, M.; Eldridge, G. R.; Hu, J. F. *J. Nat. Prod.* **2005**, *68*, 122.
- (8) Ngantchou, I.; Nyasse, B.; Denier, C.; Blonski, C.; Hannaert, V.; Schneider, B. *Bioorg. Med. Chem. Lett.* **2010**, *20*, 3495.
- (9) Williams, R. B.; Hu, J. F.; Olson, K. M.; Norman, V. L.; Goering, M. G.; O'Neil-Johnson, M.; Eldridge, G. R.; Starks, C. M. *J. Nat. Prod.* **2010**, *73*, 1008.
- (10) (a) Uchida, R.; Kim, Y. P.; Nagamitsu, T.; Tomoda, H.; Omura, S. *J. Antibiot.* **2006**, *59*, 338. (b) Roll, D. M.; Barbieri, L. R.; Bigelis, R.; McDonald, L. A.; Arias, D. A.; Chang, L. P.; Singh, M. P.; Luckman, S. W.; Berrodin, T. J.; Yudit, M. R. *J. Nat. Prod.* **2009**, *72*, 1944.
- (11) Cane, D. E.; Ikeda, H. *Acc. Chem. Res.* **2012**, *45*, 463.
- (12) Takada, K.; Kajiwara, H.; Imamura, N. *J. Nat. Prod.* **2010**, *73*, 698.
- (13) (a) Ding, L.; Munch, J.; Goerls, H.; Maier, A.; Fiebig, H. H.; Lin, W. H.; Hertweck, C. *Bioorg. Med. Chem. Lett.* **2010**, *20*, 6685. (b) Ding, L.; Maier, A.; Fiebig, H. H.; Lin, W. H.; Hertweck, C. *Org. Biomol. Chem.* **2011**, *9*, 4029.
- (14) (a) Wang, F.; Tian, X.; Huang, C.; Li, Q.; Zhang, S. *J. Antibiot.* **2011**, *64*, 189. (b) Niu, S.; Li, S.; Chen, Y.; Tian, X.; Zhang, H.; Zhang, G.; Zhang, W.; Yang, X.; Zhang, S.; Ju, J.; Zhang, C. *J. Antibiot.* **2011**, *64*, 711. (c) Li, S.; Tian, X.; Niu, S.; Zhang, W.; Chen, Y.; Zhang, H.; Yang, X.; Zhang, W.; Li, W.; Zhang, S.; Ju, J.; Zhang, C. *Mar. Drugs* **2011**, *9*, 1428. (d) Huang, H.; Yao, Y.; He, Z.; Yang, T.; Ma, J.; Tian, X.; Li, Y.; Huang, C.; Chen, X.; Li, W.; Zhang, S.; Zhang, C.; Ju, J. *J. Nat. Prod.* **2011**, *74*, 2122. (e) Huang, H.; Yang, T.; Ren, X.; Liu, J.; Song, Y.; Sun, A.; Ma, J.; Wang, B.; Zhang, Y.; Huang, C.; Zhang, C.; Ju, J. *J. Nat. Prod.* **2012**, *75*, 202.
- (15) (a) Rohmer, M. *Nat. Prod. Rep.* **1999**, *16*, 565. (b) Rohdich, F.; Kis, K.; Bacher, A.; Eisenreich, W. *Curr. Opin. Chem. Biol.* **2001**, *5*, 535. (c) Mizioro, H. M. *Arch. Biochem. Biophys.* **2011**, *505*, 131. (d) Hecht, S.; Eisenreich, W.; Adam, P.; Amslinger, S.; Kis, K.; Bacher, A.; Arigoni, D.; Rohdich, F. *Proc. Natl. Acad. Sci. U.S.A.* **2001**, *98*, 14837. (e) Grawert, T.; Span, I.; Bacher, A.; Groll, M. *Angew. Chem., Int. Ed.* **2010**, *49*, 8802.
- (16) Kawasaki, T.; Kuzuyama, T.; Furihata, K.; Itoh, N.; Seto, H.; Dairi, T. *J. Antibiot.* **2003**, *56*, 957.
- (17) (a) Cane, D. E.; Watt, R. M. *Proc. Natl. Acad. Sci. U.S.A.* **2003**, *100*, 1547. (b) Jiang, J.; He, X.; Cane, D. E. *Nat. Chem. Biol.* **2007**, *3*, 711. (c) Nawrath, T.; Dickschat, J. S.; Muller, R.; Jiang, J.; Cane, D. E.; Schulz, S. *J. Am. Chem. Soc.* **2008**, *130*, 430. (d) Jiang, J.; Cane, D. E. *J. Am. Chem. Soc.* **2008**, *130*, 428.
- (18) (a) Lin, X.; Hopson, R.; Cane, D. E. *J. Am. Chem. Soc.* **2006**, *128*, 6022. (b) Aaron, J. A.; Lin, X.; Cane, D. E.; Christianson, D. W. *Biochemistry* **2010**, *49*, 1787.
- (19) (a) Zhao, B.; Lin, X.; Lei, L.; Lamb, D. C.; Kelly, S. L.; Waterman, M. R.; Cane, D. E. *J. Biol. Chem.* **2008**, *283*, 8183. (b) Lin, X.; Cane, D. E. *J. Am. Chem. Soc.* **2009**, *131*, 6332. (c) Zhao, B.; Lei, L.; Vassilyev, D. G.; Lin, X.; Cane, D. E.; Kelly, S. L.; Yuan, H.; Lamb, D. C.; Waterman, M. R. *J. Biol. Chem.* **2009**, *284*, 36711.
- (20) (a) Tetzlaff, C. N.; You, Z.; Cane, D. E.; Takamatsu, S.; Omura, S.; Ikeda, H. *Biochemistry* **2006**, *45*, 6179. (b) You, Z.; Omura, S.; Ikeda, H.; Cane, D. E. *J. Am. Chem. Soc.* **2006**, *128*, 6566. (c) Quaderer, R.; Omura, S.; Ikeda, H.; Cane, D. E. *J. Am. Chem. Soc.* **2006**, *128*, 13036. (d) Seo, M. J.; Zhu, D.; Endo, S.; Ikeda, H.; Cane, D. E. *Biochemistry* **2011**, *50*, 1739. (e) Zhu, D.; Seo, M. J.; Ikeda, H.; Cane, D. E. *J. Am. Chem. Soc.* **2011**, *133*, 2128.
- (21) Chou, W. K.; Fanzizza, I.; Uchiyama, T.; Komatsu, M.; Ikeda, H.; Cane, D. E. *J. Am. Chem. Soc.* **2010**, *132*, 8850.
- (22) (a) Yu, F.; Zaleta-Rivera, K.; Zhu, X.; Huffman, J.; Millet, J. C.; Harris, S. D.; Yuen, G.; Li, X. C.; Du, L. *Antimicrob. Agents Chemother.* **2007**, *51*, 64. (b) Lou, L.; Qian, G.; Xie, Y.; Hang, J.; Chen, H.; Zaleta-Rivera, K.; Li, Y.; Shen, Y.; Dussault, P. H.; Liu, F.; Du, L. *J. Am. Chem. Soc.* **2011**, *133*, 643.
- (23) Grawert, T.; Groll, M.; Rohdich, F.; Bacher, A.; Eisenreich, W. *Cell. Mol. Life Sci.* **2011**, *68*, 3797.
- (24) (a) Omura, S.; Ikeda, H.; Ishikawa, J.; Hanamoto, A.; Takahashi, C.; Shinose, M.; Takahashi, Y.; Horikawa, H.; Nakazawa, H.; Osonoe, T.; Kikuchi, H.; Shiba, T.; Sakaki, Y.; Hattori, M. *Proc. Natl. Acad. Sci. U.S.A.* **2001**, *98*, 12215. (b) Ikeda, H.; Ishikawa, J.; Hanamoto, A.; Shinose, M.; Kikuchi, H.; Shiba, T.; Sakaki, Y.; Hattori, M.; Omura, S. *Nat. Biotechnol.* **2003**, *21*, 526.
- (25) (a) Tarshis, L. C.; Yan, M.; Poulter, C. D.; Sacchetti, J. C. *Biochemistry* **1994**, *33*, 10871. (b) Gabelli, S. B.; McLellan, J. S.; Montalvetti, A.; Oldfield, E.; Docampo, R.; Amzel, L. M. *Proteins* **2006**, *62*, 80.
- (26) De Schrijver, A.; De Mot, R. *Microbiology* **1999**, *145*, 1287.
- (27) (a) Wilson, D. J.; Xue, Y.; Reynolds, K. A.; Sherman, D. H. *J. Bacteriol.* **2001**, *183*, 3468–3475. (b) Kuscer, E.; Coates, N.; Challis, I.; Gregory, M.; Wilkinson, B.; Sheridan, R.; Petkovic, H. *J. Bacteriol.* **2007**, *189*, 4756. (c) Laureti, L.; Song, L.; Huang, S.; Corre, C.; Leblond, P.; Challis, G. L.; Aigle, B. *Proc. Natl. Acad. Sci. U.S.A.* **2011**, *108*, 6258.
- (28) (a) Ferraro, D. J.; Gakhar, L.; Ramaswamy, S. *Biochem. Biophys. Res. Commun.* **2005**, *338*, 175. (b) Schneider, D.; Schmidt, C. L. *Biochim. Biophys. Acta* **2005**, *1710*, 1.
- (29) Lim, H. K.; Chung, E. J.; Kim, J. C.; Choi, G. J.; Jang, K. S.; Chung, Y. R.; Cho, K. Y.; Lee, S. W. *Appl. Environ. Microbiol.* **2005**, *71*, 7768.
- (30) Arand, M.; Hallberg, B. M.; Zou, J.; Bergfors, T.; Oesch, F.; van der Werf, M. J.; de Bont, J. A.; Jones, T. A.; Mowbray, S. L. *EMBO J.* **2003**, *22*, 2583.
- (31) Smanski, M. J.; Yu, Z.; Casper, J.; Lin, S.; Peterson, R. M.; Chen, Y.; Wendt-Pienkowski, E.; Rajski, S. R.; Shen, B. *Proc. Natl. Acad. Sci. U.S.A.* **2011**, *108*, 13498.
- (32) (a) Kuzuyama, T.; Seto, H. *Nat. Prod. Rep.* **2003**, *20*, 171. (b) Durr, C.; Schnell, H. J.; Luzhetskyy, A.; Murillo, R.; Weber, M.; Welzel, K.; Vente, A.; Bechthold, A. *Chem. Biol.* **2006**, *13*, 365.
- (33) Stec, E.; Pistorius, D.; Muller, R.; Li, S. M. *ChemBioChem* **2011**, *12*, 1724.
- (34) (a) Saikia, S.; Parker, E. J.; Koulman, A.; Scott, B. *FEBS Lett.* **2006**, *580*, 1625. (b) Li, S. M. *Nat. Prod. Rep.* **2010**, *27*, 57.
- (35) (a) Ames, B. D.; Liu, X.; Walsh, C. T. *Biochemistry* **2010**, *49*, 8564. (b) Gao, X.; Chooi, Y. H.; Ames, B. D.; Wang, P.; Walsh, C. T.; Tang, Y. *J. Am. Chem. Soc.* **2011**, *133*, 2729.
- (36) Meyer, A.; Wursten, M.; Schmid, A.; Kohler, H. P.; Witholt, B. *J. Biol. Chem.* **2002**, *277*, 34161.
- (37) Balibar, C. J.; Walsh, C. T. *Biochemistry* **2006**, *45*, 15444.
- (38) Li, S.; Finefield, J. M.; Sunderhaus, J. D.; McAfoos, T. J.; Williams, R. M.; Sherman, D. H. *J. Am. Chem. Soc.* **2012**, *134*, 788.
- (39) Itoh, T.; Tokunaga, K.; Matsuda, Y.; Fujii, I.; Abe, I.; Ebizuka, Y.; Kushiro, T. *Nat. Chem.* **2010**, *2*, 858.
- (40) (a) Brautaset, T.; Sletta, H.; Degnes, K. F.; Sekurova, O. N.; Bakke, I.; Volokhan, O.; Andreassen, T.; Ellingsen, T. E.; Zotchev, S. B. *Appl. Environ. Microbiol.* **2011**, *77*, 6636. (b) Carmody, M.; Murphy, B.; Byrne, B.; Power, P.; Rai, D.; Rawlings, B.; Caffrey, P. *J. Biol. Chem.* **2005**, *280*, 34420.
- (41) (a) Sambrook, J.; Fritsch, E. F.; Maniatis, T. *Molecular Cloning: A Laboratory Manual*, 2nd ed.; Cold Spring Harbor Laboratory Press: Cold Spring Harbor, NY, USA, 1989. (b) Kieser, T.; Bibb, M. J.; Buttner, M. J.; Chater, K. F.; Hopwood, D. A. *Practical Streptomyces Genetics*; John Innes Foundation: Colney, Norwich, U.K., 2000.
- (42) (a) Gust, B.; Challis, G. L.; Fowler, K.; Kieser, T.; Chater, K. F. *Proc. Natl. Acad. Sci. U.S.A.* **2003**, *100*, 1541. (b) Gust, B.; Chandra, G.; Jakimowicz, D.; Yuqing, T.; Bruton, C. J.; Chater, K. F. *Adv. Appl. Microbiol.* **2004**, *54*, 107.
- (43) Bradford, M. M. *Anal. Biochem.* **1976**, *72*, 248.